STATISTICS, OPTIMIZATION AND INFORMATION COMPUTING
Stat., Optim. Inf. Comput., Vol. **14**, July 2025, pp 130–143.
Published online in International Academic Press (www.IAPress.org)

Hybrid Euler method and Pontryagin Principle in Fractional Dengue Model with Sex Classification and Optimal Controls

Faishal Farrel Herdicho [1], Fatmawati [1,*], Cicik Alfiniyah [1], Chidozie Williams Chukwu [2]

[1] *Department of Mathematics, Faculty of Science and Technology, Universitas Airlangga, Surabaya, 60115, Indonesia*
[2] *Department of Mathematical Sciences, DePaul University, Chicago, IL 60614, USA*

Abstract This study develops a fractional epidemiological model to investigate the dynamics of dengue transmission, incorporating biological and behavioral differences between male and female human populations. The model utilizes fractional calculus to capture memory effects, which are essential for understanding the long-term behavior of infectious diseases. Control variables representing fumigation and preventive measures are introduced to evaluate intervention strategies, formulating a fractional optimal control problem. To solve the model, Euler's method is employed for numerical approximation of the fractional differential equations, while Pontryagin's Minimum Principle and a forward-backward numerical approach are applied to determine optimal strategies. Parameter estimation is conducted using the least-squares fitting method based on cumulative dengue hemorrhagic fever (DHF) case data from West Java Province, Indonesia from 2014 to 2023. The estimation yields a Mean Absolute Percentage Error (MAPE) of 4.32% for males and 4.50% for females, with an overall fit of 4.41%. As one of the key parameters affecting basic reproduction number, proportion of additional immunity levels among females is simulated to examine its influence on infection outcomes. The results show that increasing this parameter reduces female infections, which subsequently lowers vector transmission and indirectly decreases male infections. In the control simulation, lower fractional orders enhance the efficiency of system dynamics, leading to faster convergence towards the desired infection reduction. Additionally, the cost-effectiveness analysis indicates that the implementation of a combined strategy, incorporating both fumigation and preventive measures, provides the most efficient intervention.

Keywords Dengue, Euler's Method, Fractional Model, Optimal Control, Parameter Estimation, Sex Classification

AMS 2010 subject classifications 34A08, 49M99, 90C32

DOI: 10.19139/soic-2310-5070-2393

1. Introduction

Dengue is a mosquito-borne viral infection primarily transmitted to humans through the bite of infected *Aedes aegypti* mosquitoes, posing a significant threat to nearly half of the world's population. It is estimated that 100–400 million infections occur annually, predominantly in tropical and subtropical regions, particularly in densely populated urban and semi-urban areas. While many infections are asymptomatic or result in mild symptoms, severe cases such as dengue hemorrhagic fever and dengue shock syndrome can lead to life-threatening complications and significant mortality. Effective prevention and control efforts rely heavily on vector control strategies, as there is currently no specific antiviral treatment available for dengue or its severe forms. Early diagnosis, coupled with timely access to adequate medical care, has proven essential in reducing the fatality rates of severe cases, emphasizing the importance of strengthening public health systems and community awareness in endemic regions [1].

*Correspondence to: Fatmawati (Email: fatmawati@fst.unair.ac.id). Department of Mathematics, Faculty of Science and Technology, Universitas Airlangga, Jln. Dr. Ir. H. Soekarno, Mulyorejo, Surabaya, Indonesia (60115).

ISSN 2310-5070 (online) ISSN 2311-004X (print)

In this study, we focus on developing a mathematical model for the transmission of dengue fever that incorporates a classification by sex. This differentiation is motivated by observed biological and behavioral variations between males and females in terms of susceptibility to infection, immune response, and exposure to *Aedes aegypti* mosquitoes. Males of many species, including humans, have been found to be more susceptible than females to infections caused by parasites, fungi, bacteria, and viruses. One proximate cause of these sex differences in infection is the variation in endocrine-immune interactions. Specifically, sex steroids such as androgens in males and estrogens in females modulate several aspects of host immunity, potentially making males more vulnerable to infections [2]. Incorporating these sex-specific variations into a mathematical model allows for a more detailed understanding of dengue transmission dynamics and facilitates the design of more effective and targeted interventions, considering these physiological and behavioral differences.

Moreover, the model is formulated within the framework of fractional calculus, which accounts for the memory effects inherent in infectious diseases, such as dengue. Unlike traditional integer-order models, which only consider the present state of a system, fractional-order models incorporate the influence of past states, making them particularly well-suited for diseases where historical dynamics significantly impact current transmission processes. This is especially relevant in the case of dengue, where factors such as previous exposure to the virus, environmental conditions, and immune system responses can influence the progression and spread of the disease. Fractional derivatives capture these memory effects, offering a more accurate and realistic representation of disease dynamics compared to classical models [3].

To enhance the model's practical relevance, we also incorporate an optimal control problem focusing on two intervention strategies: fumigation to reduce vector populations and preventive measures to limit human exposure. These control measures are incorporated as time-dependent variables, and their optimal implementation is determined by minimizing a cost functional that balances the effectiveness of interventions with their associated costs. By framing the problem in this way, we seek to identify strategies that provide the greatest reduction in dengue transmission at the lowest cost, ensuring both efficiency and sustainability in real-world applications.

The numerical simulation of this model is a challenging task due to the complexities introduced by fractional-order dynamics and the optimization process. Researchers such as [4, 5, 6, 7] have explored fractional-order models in their studies, while [8, 9, 10, 11] have investigated optimal control frameworks. Additionally, [12, 13, 14, 15, 16] have focused on integrating optimal control with fractional-order models. To address these challenges, we adopt a hybrid numerical scheme that combines the forward-backward iterative method with Euler's algorithm. This method ensures accurate solutions to the fractional differential equations governing the system while efficiently solving the optimal control problem. By combining sex-classified fractional modeling with optimal control and advanced numerical techniques, this study provides a novel framework for analyzing dengue transmission dynamics and guiding effective intervention strategies.

2. Fractional Model Formulation

In this section, we present a model of dengue infection with sex-based classification in the human population. This classification is emphasized to highlight the increased susceptibility of males to the virus. In this study, we restrict the model to a basic $SIR - SI$ framework and only considering a single virus serotype, which excludes the possibility of reinfection. The notation and description of each populations and parameters are provided in Table 1 and Table 2.

Therefore, we present the transmission dynamics of the dengue transmission model is illustrated in the diagram presented in Figure 1. This diagram serves as a conceptual representation of the interactions and transitions among the various compartments in the system.

Table 1. Compartments description.

Compartments	Description
S_v	Number of susceptible mosquito population
I_v	Number of infected mosquito population
S_m	Number of susceptible male human population
S_f	Number of susceptible female human population
I_m	Number of infected male human population
I_f	Number of infected female human population
R_m	Number of recovery male human population
R_f	Number of recovery female human population

Table 2. Parameters description.

Parameters	Description
Λ_v	Growth rate of mosquito population
$\Lambda_{m,f}$	Growth rate of (m = male, f = female) human population
β_v	Transmission rate from human to mosquito
β_h	Transmission rate from mosquito to human
$(1-\gamma)$	Proportion of additional immunity level for female human population
μ_v	Natural death rate of mosquito population
$\mu_{m,f}$	Natural death rate of (m = male, f = female) human population
$\tau_{m,f}$	Dengue mortality rate of (m = male, f = female) human population
$\theta_{m,f}$	Recovery rate of (m = male, f = female) human population

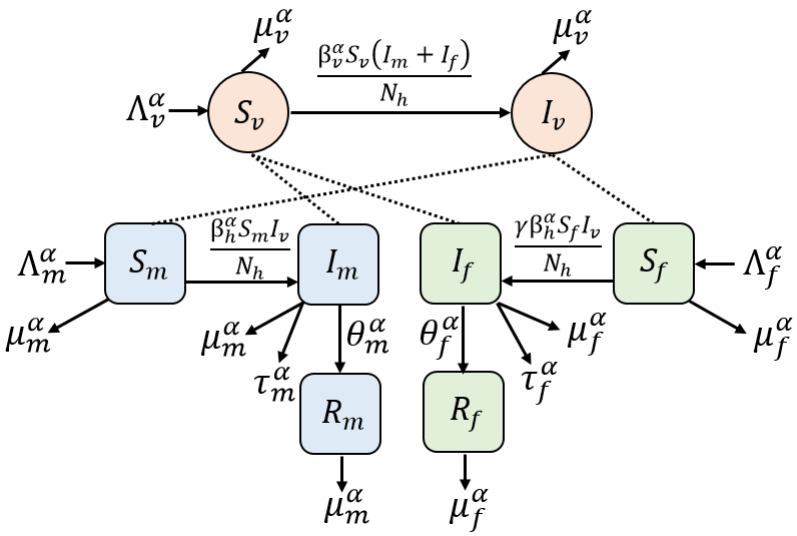

Figure 1. Dengue transmission diagram.

Based on the transmission diagram in Figure 1, the system of fractional differential equations for the mathematical model of dengue spread is formulated as follows:

$$\begin{aligned}
{}^{C}D_t^{\alpha} S_v &= \Lambda_v^{\alpha} - \frac{\beta_v^{\alpha}(I_m + I_f)S_v}{N_h} - \mu_v^{\alpha} S_v, \\
{}^{C}D_t^{\alpha} I_v &= \frac{\beta_v^{\alpha}(I_m + I_f)S_v}{N_h} - \mu_v^{\alpha} I_v, \\
{}^{C}D_t^{\alpha} S_m &= \Lambda_m^{\alpha} - \frac{\beta_h^{\alpha} I_v S_m}{N_h} - \mu_m^{\alpha} S_m, \\
{}^{C}D_t^{\alpha} S_f &= \Lambda_f^{\alpha} - \gamma\frac{\beta_h^{\alpha} I_v S_f}{N_h} - \mu_f^{\alpha} S_f, \\
{}^{C}D_t^{\alpha} I_m &= \frac{\beta_h^{\alpha} I_v S_m}{N_h} - (\mu_m^{\alpha} + \tau_m^{\alpha} + \theta_m^{\alpha}) I_m, \\
{}^{C}D_t^{\alpha} I_f &= \gamma\frac{\beta_h^{\alpha} I_v S_f}{N_h} - (\mu_f^{\alpha} + \tau_f^{\alpha} + \theta_f^{\alpha}) I_f, \\
{}^{C}D_t^{\alpha} R_m &= \theta_m^{\alpha} I_m - \mu_m^{\alpha} R_m, \\
{}^{C}D_t^{\alpha} R_f &= \theta_f^{\alpha} I_f - \mu_f^{\alpha} R_f,
\end{aligned} \tag{1}$$

with ${}^{C}D_t^{\alpha}$ represents the Caputo fractional derivative with $\alpha \in (0, 1]$, which accounts for memory effects in disease dynamics.

The variables S_v, I_v, S_m, S_f, I_m, and I_f are all non-negative, ensuring biological feasibility. The total human population is given by $N_h = S_m + S_f + I_m + I_f + R_m + R_f \geq 0$ and the total mosquito population is $N_v = S_v + I_v \geq 0$. Additionally, all parameters defined in the model are positive, with $0 \leq \gamma \leq 1$ as proportion and Λ_v^{α}, Λ_m^{α}, Λ_f^{α}, β_v^{α}, β_h^{α}, μ_v^{α}, μ_m^{α}, μ_f^{α}, θ_m^{α}, θ_f^{α}, τ_m^{α}, and $\tau_f^{\alpha} > 0$. The fractional order α ensures dimensional consistency, with the growth rates $\Lambda_v^{\alpha}, \Lambda_m^{\alpha}, \Lambda_f^{\alpha}$ having dimensions of $\frac{\text{population}}{\text{time}^{\alpha}}$, and other rate parameters measured in $\frac{1}{\text{time}^{\alpha}}$.

3. Euler's Method

Euler's method is a fundamental numerical algorithm used to solve fractional differential equations. Based on explanations from [13], the steps for implementing Euler's method in this context are outlined below.

Consider the initial value problem (IVP):

$${}^{C}D_t^{\alpha} y(t) = f\left(t, y\left(t\right)\right), \qquad 0 < \alpha \leq 1, \tag{2}$$

with the initial condition:

$$y(0) = y_0, \qquad 0 < t \leq t_f,$$

where $f\left(t, y\left(t\right)\right)$ is a given function that satisfies certain smoothness conditions [17].

The function $y(t)$, known as the exact solution, that satisfies the IVP in Equation (2). However, the numerical procedure aims to approximate $y(t)$ at discrete points within the interval of interest. The interval $[0, t_f]$ is divided into n equal intervals $[t_j, t_(j+1)]$, each of size $h = \frac{t_f}{n}$, with nodes $t_j = jh$, for $j = 0, 1, \ldots, n$.

To derive a numerical approximation, we first rewrite the fractional differential equation as an equivalent Volterra integral equation [18] by applying the fractional integral operator ${}^{C}D_t^{-\alpha}$ to both sides of Equation (2):

$$y(t) = y_0 + {}^{C}D_t^{-\alpha} f\left(t, y\left(t\right)\right).$$

According to [17], ${}^{C}D_t^{-\alpha} f\left(t, y\left(t\right)\right)$ is then approximated by a left fractional rectangular formula in such a way:

$$y\left(t_{n+1}\right) = y_0 + \frac{h^{\alpha}}{\Gamma(\alpha+1)} \sum_{j=0}^{n} b_{j,n+1} f\left(t_j, y\left(j\right)\right),$$

where the coefficients $b_{j,n+1}$ are defined as $b_{j,n+1} = (n+1-j)^{\alpha} - (n-j)^{\alpha}$.

4. Fractional Parameter Estimation

In this section, we estimate the parameters of the fractional-order model (1). First, we collect data from [19, 20, 21, 22], which includes DHF cases in humans, DHF mortality in humans, total human populations, and life expectancy in West Java Province, Indonesia, categorized by sex from 2014 to 2023. To estimate parameters, we use cumulative DHF case data for each year from 2014 to 2023. The parameter estimation follows the least-squares fitting method [23], applied to the fractional-order model. Some parameters will be estimated based on geographical data, namely $\mu_v,\ \mu_m,\ \mu_f, \Lambda_m, \Lambda_f, \tau_m$, and τ_f. The natural death rate is derived from the inverse of life expectancy. According to [24], the average life expectancy of Aedes mosquitoes is 25 days. The average life expectancy for male and female human populations is 71.048 years and 74.864 years, respectively [22]. Thus, we obtain $\mu_v = 14.6$, $\mu_m = 0.0141$, and $\mu_f = 0.0134$ per year. The human growth rate is calculated as the product of the total population and the natural death rate. Using the data from [21, 22], we estimate $\Lambda_m = 328,323$ and $\Lambda_f = 301,673$ individuals per year. The DHF mortality rate is approximated using the Case Fatality Rate (CFR), which represents the proportion of infected individuals who die from DHF. Based on data from [20], we estimate $\tau_m = 0.0068$ and $\tau_f = 0.0087$ per year.

The remaining parameters, including the fractional-order, are estimated by minimizing the following objective function:

$$\min_{\Lambda_v,\beta_v,\beta_h,\gamma,\theta_m,\theta_f,\alpha} \sum_{i=0}^{t_f} \left(\left(I_{m_i} - I_{m_i}^{data}\right)^2 + \left(I_{f_i} - I_{f_i}^{data}\right)^2 \right),$$

where t_f is the final time, $I_{m_i}^{data}$ and $I_{f_i}^{data}$ are the cumulative DHF cases for male and female populations, respectively, while I_{m_i} and I_{f_i} are the corresponding numerical solutions of the fractional-order model for $i = 0, 1, 2, \ldots, t_f$.

For the estimation process, the initial value, lower bound, upper bound, and estimated parameters value are presented in Table 3, while the comparison between the reported data and the model solution is shown in Figure 2.

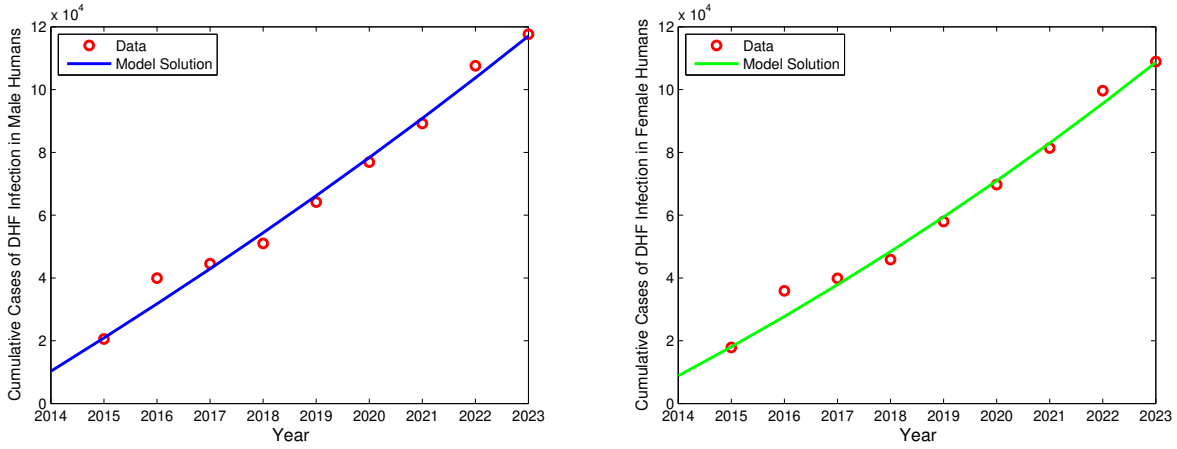

Figure 2. Comparison between data and model solution.

Based on the estimation results, the Mean Absolute Percentage Error (MAPE) between the data and the model solution is 4.32% for the male population and 4.50% for the female population. The overall average MAPE is 4.41%, indicating a good fit of the fractional-order model to the data.

Table 3. Estimated values of model parameters.

Parameters	Lower Bound	Upper Bound	Initial Value	Value (Year)	Source
α	10^{-3}	1	0.9	0.9718	Fitted
Λ_m^α	-	-	-	$328,323^\alpha$	Estimated
Λ_f^α	-	-	-	$301,673^\alpha$	Estimated
μ_m^α	-	-	-	0.0141^α	Estimated
μ_f^α	-	-	-	0.0134^α	Estimated
μ_v^α	-	-	-	14.6^α	Estimated
τ_m^α	-	-	-	0.0068^α	Estimated
τ_f^α	-	-	-	0.0087^α	Estimated
β_h^α	10^{-3}	1	0.5	1^α	Fitted
β_v^α	10^{-3}	1	0.5	0.9997^α	Fitted
γ	10^{-3}	1	0.5	0.9826	Fitted
θ_m^α	10^{-3}	1	0.5	0.0165^α	Fitted
θ_f^α	10^{-3}	1	0.5	0.0010^α	Fitted
Λ_v^α	10^8	10^{10}	10^9	$(10^9)^\alpha$	Fitted

5. Sensitivity Analysis

In this section, we conduct a sensitivity analysis to determine which parameters have a significant influence on the basic reproduction number (R_0). Following the methodology outlined in [25], we employ the sensitivity index to quantify the impact of each parameter.

The basic reproduction number is derived using the Next-Generation Matrix method [26], which involves computing the spectral radius of the Jacobian matrix evaluated at the disease-free equilibrium. This method ensures an accurate representation of the transmission potential of the infection within the population. The expression for R_0 is given by:

$$R_0 = \sqrt{\frac{\beta_h \beta_v \Lambda_v \mu_m \mu_f \left(\Lambda_m m_2 \mu_f + \gamma \Lambda_f m_1 \mu_m\right)}{m_1 m_2 \mu_v^2 (\Lambda_m \mu_f + \Lambda_f \mu_m)^2}},$$

where $m_1 = (\theta_m + \tau_m + \mu_m)$ and $m_2 = (\theta_f + \tau_f + \mu_f)$.

The sensitivity index of R_0 with respect to a parameter p is defined as:

$$\Upsilon_p^{R_0} = \frac{\partial R_0}{\partial p} \times \frac{p}{R_0}.$$

This index measures the relative change in R_0 resulting from a small relative change in the parameter p. A positive sensitivity index indicates that an increase in p leads to an increase in R_0, whereas a negative value suggests an inverse relationship. Using the parameter values listed in Table 3, we compute the sensitivity indices and present the results in Table 4.

Table 4. Parameter sensitivity index.

Parameters	Sensitivity Index	Parameters	Sensitivity Index	Parameters	Sensitivity Index
Λ_v	0.50	μ_v	-1.00	θ_m	-0.09
Λ_m	-0.31	μ_m	0.24	θ_f	-0.01
Λ_f	-0.19	μ_f	0.02	γ	0.30
β_v	0.50	τ_m	-0.04		
β_h	0.50	τ_f	-0.11		

The largest and smallest values of the sensitivity index indicate the most influential parameters affecting changes in R_0, namely μ_v, Λ_v, β_v, β_h, Λ_m, and γ. Furthermore, to analyze the impact of parameter variations, we conduct simulations by selecting some values of γ to observe its effect on infection outcomes. The parameter $(1-\gamma)$ represents the proportion of additional immunity level for the female human population. By varying γ, we can assess how changes in immunity levels among females influence the overall disease spread, peak infection levels, and total number of infected individuals over time. These insights are essential for designing gender-targeted policies, considering that biological and behavioral differences may affect immune responses and disease progression.

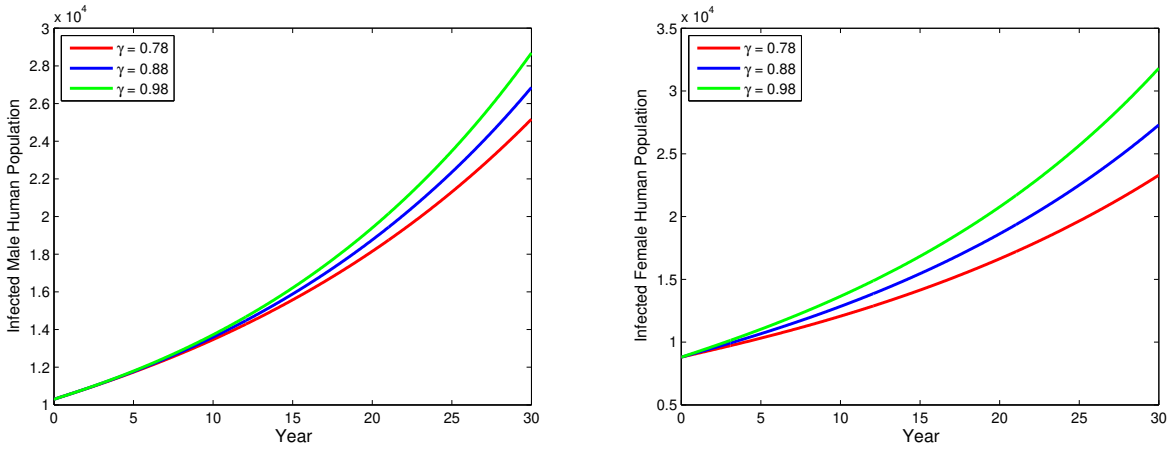

Figure 3. Impact of γ on the Infected Population.

Based on the Figure 3, it can be concluded that although γ directly influences the infected female population, its variation also indirectly affects the infected male population. As the value of γ increases, the proportion of females receiving additional immunity $(1-\gamma)$ decreases, leading to a rise in the number of infected females. This, in turn, increases the number of infected vectors (mosquitoes), ultimately resulting in a higher number of infected males. Conversely, when the proportion of immune females increases, the number of infected mosquitoes declines, leading to a reduction in male infections. Thus, controlling γ is not only crucial for reducing infections among females but also has a cascading effect on male infections through vector-mediated transmission dynamics.

6. Fractional Optimal Control Problem

In this section, we extend the model in Equation (1) by introducing control variables. Specifically, the controls u_1 and u_2 represent fumigation efforts and preventive measures, respectively. The primary objective of fumigation efforts is to reduce the population of vectors, such as mosquitoes, that act as carriers for the disease. Preventive measures can include public awareness campaigns, personal protection, or environmental management to reduce human exposure to vectors. The modified fractional differential system in Equation (1) with these control variables

is formulated as follows:

$$\begin{aligned}
{}^{C}D_t^{\alpha} S_v &= \Lambda_v^{\alpha} - \frac{\beta_v^{\alpha}(I_m + I_f)S_v}{N_h} - \mu_v^{\alpha} S_v - \theta^{\alpha} u_1 S_v, \\
{}^{C}D_t^{\alpha} I_v &= \frac{\beta_v^{\alpha}(I_m + I_f)S_v}{N_h} - \mu_v^{\alpha} I_v - \theta^{\alpha} u_1 I_v, \\
{}^{C}D_t^{\alpha} S_m &= \Lambda_m^{\alpha} - (1-u_2)\frac{\beta_h^{\alpha} I_v S_m}{N_h} - \mu_m^{\alpha} S_m, \\
{}^{C}D_t^{\alpha} S_f &= \Lambda_f^{\alpha} - (1-u_2)\gamma\frac{\beta_h^{\alpha} I_v S_f}{N_h} - \mu_f^{\alpha} S_f, \\
{}^{C}D_t^{\alpha} I_m &= (1-u_2)\frac{\beta_h^{\alpha} I_v S_m}{N_h} - (\mu_m^{\alpha} + \tau_m^{\alpha} + \theta_m^{\alpha}) I_m, \\
{}^{C}D_t^{\alpha} I_f &= (1-u_2)\gamma\frac{\beta_h^{\alpha} I_v S_f}{N_h} - (\mu_f^{\alpha} + \tau_f^{\alpha} + \theta_f^{\alpha}) I_f, \\
{}^{C}D_t^{\alpha} R_m &= \theta_m^{\alpha} I_m - \mu_m^{\alpha} R_m, \\
{}^{C}D_t^{\alpha} R_f &= \theta_f^{\alpha} I_f - \mu_f^{\alpha} R_f,
\end{aligned} \tag{3}$$

where θ^{α} represents the effectiveness rate of fumigation, with a dimension of $\frac{1}{\text{time}^{\alpha}}$. Both control variables are constrained within $u_1, u_2 \in [0,1]$. It is important to note that the system in Equation (3) reverts to the model without control in Equation (1) when $u_1 = u_2 = 0$.

The goal of this fractional optimal control problem is to minimize the number of infected male and female humans, as well as infected mosquitoes, while simultaneously considering the costs associated with implementing control strategies. The objective functional is defined as:

$$\min \mathcal{J}(I_v, I_m, I_f, u_1, u_2) = \int_0^{t_f} A_1 I_v + A_2 I_m + A_3 I_f + \frac{1}{2} A_4 u_1^2 + \frac{1}{2} A_5 u_2^2 \; dt,$$

where A_1, A_2, A_3 are weighting constants for the infected populations I_v, I_m, and I_f, and A_4, A_5 are cost coefficients for the controls u_1 dan u_2 respectively, These constants satisfy $0 < A_1, A_2, A_3, A_4, A_5 < \infty$.

To solve this fractional optimal control problem, we use Pontryagin's Minimum Principle (PMP) for fractional optimal control method [13, 27]. The Hamiltonian of the system is given by:

$$\begin{aligned}
H &= A_1 I_v + A_2 I_m + A_3 I_f + \frac{1}{2} A_4 u_1^2 + \frac{1}{2} A_5 u_2^2 + \\
&\lambda_1 \left(\Lambda_v^{\alpha} - \frac{\beta_v^{\alpha}(I_m + I_f)S_v}{N_h} - \mu_v^{\alpha} S_v - \theta^{\alpha} u_1 S_v \right) + \lambda_2 \left(\frac{\beta_v^{\alpha}(I_m + I_f)S_v}{N_h} - \mu_v^{\alpha} I_v - \theta^{\alpha} u_1 I_v \right) + \\
&\lambda_3 \left(\Lambda_m^{\alpha} - (1-u_2)\frac{\beta_h^{\alpha} I_v S_m}{N_h} - \mu_m^{\alpha} S_m \right) + \lambda_4 \left(\Lambda_f^{\alpha} - (1-u_2)\gamma\frac{\beta_h^{\alpha} I_v S_f}{N_h} - \mu_f^{\alpha} S_f \right) + \\
&\lambda_5 \left((1-u_2)\frac{\beta_h^{\alpha} I_v S_m}{N_h} - (\mu_m^{\alpha} + \tau_m^{\alpha} + \theta_m^{\alpha}) I_m \right) + \lambda_6 \left((1-u_2)\gamma\frac{\beta_h^{\alpha} I_v S_f}{N_h} - (\mu_f^{\alpha} + \tau_f^{\alpha} + \theta_f^{\alpha}) S_f \right) + \\
&\lambda_7 \left(\theta_m^{\alpha} I_m - \mu_m^{\alpha} R_m \right) + \lambda_8 \left(\theta_f^{\alpha} I_f - \mu_f^{\alpha} R_f \right).
\end{aligned}$$

The optimality conditions from PMP ensure that the controls are given by:

$$\begin{aligned}
u_1^* &= \min\left(\max\left(0, \frac{\theta^{\alpha}(\lambda_1 S_v + \lambda_2 I_v)}{A_4} \right), 1 \right) \\
u_2^* &= \min\left(\max\left(0, \frac{(\lambda_5 - \lambda_3)\beta_h^{\alpha} I_v S_m + (\lambda_6 - \lambda_4)\gamma\beta_h^{\alpha} I_v S_f}{A_5 N_h} \right), 1 \right)
\end{aligned}$$

while the adjoint system asserts that the co-state variables $\lambda_i(t)$, $i = 1, 2, \ldots, 8$ satisfy

$$
\begin{aligned}
{}_tD^{\alpha}_{t_f}\lambda_1 &= (\lambda_1-\lambda_2)\frac{\beta_v^{\alpha}(I_m+I_f)}{N_h}+\lambda_1(\mu_v^{\alpha}+\theta^{\alpha}u_1),\\
{}_tD^{\alpha}_{t_f}\lambda_2 &= -A_1+(\lambda_3-\lambda_5)(1-u_2)\frac{\beta_h^{\alpha}S_m}{N_h}+(\lambda_4-\lambda_6)(1-u_2)\gamma\frac{\beta_h^{\alpha}S_f}{N_h}+\lambda_2(\mu_v^{\alpha}+\theta^{\alpha}u_1),\\
{}_tD^{\alpha}_{t_f}\lambda_3 &= (\lambda_2-\lambda_1)\frac{\beta_v^{\alpha}(I_m+I_f)S_v}{N_h^2}+(\lambda_3-\lambda_5)(1-u_2)\frac{\beta_h^{\alpha}I_v(N_h-S_m)}{N_h^2}+\\
&\quad (\lambda_6-\lambda_4)(1-u_2)\gamma\frac{\beta_h^{\alpha}I_vS_f}{N_h^2}+\lambda_3\mu_m^{\alpha},\\
{}_tD^{\alpha}_{t_f}\lambda_4 &= (\lambda_2-\lambda_1)\frac{\beta_v^{\alpha}(I_m+I_f)S_v}{N_h^2}+(\lambda_5-\lambda_3)(1-u_2)\frac{\beta_h^{\alpha}I_vS_m}{N_h^2}+\\
&\quad (\lambda_4-\lambda_6)(1-u_2)\gamma\frac{\beta_h^{\alpha}I_v(N_h-S_f)}{N_h^2}+\lambda_4\mu_f^{\alpha},\\
{}_tD^{\alpha}_{t_f}\lambda_5 &= -A_2+(\lambda_1-\lambda_2)\frac{\beta_v^{\alpha}S_v(N_h-(I_m+I_f))}{N_h^2}+(\lambda_5-\lambda_3)(1-u_2)\frac{\beta_h^{\alpha}I_vS_m}{N_h^2}+\\
&\quad (\lambda_6-\lambda_4)(1-u_2)\gamma\frac{\beta_h^{\alpha}I_vS_f}{N_h^2}+(\lambda_5-\lambda_7)\theta_m^{\alpha}+\lambda_5(\mu_m^{\alpha}+\tau_m^{\alpha}),\\
{}_tD^{\alpha}_{t_f}\lambda_6 &= -A_3+(\lambda_1-\lambda_2)\frac{\beta_v^{\alpha}S_v(N_h-(I_m+I_f))}{N_h^2}+(\lambda_5-\lambda_3)(1-u_2)\frac{\beta_h^{\alpha}I_vS_m}{N_h^2}+\\
&\quad (\lambda_6-\lambda_4)(1-u_2)\gamma\frac{\beta_h^{\alpha}I_vS_f}{N_h^2}+(\lambda_6-\lambda_8)\theta_f^{\alpha}+\lambda_6(\mu_f^{\alpha}+\tau_f^{\alpha}),\\
{}_tD^{\alpha}_{t_f}\lambda_7 &= (\lambda_2-\lambda_1)\frac{\beta_v^{\alpha}(I_m+I_f)S_v}{N_h^2}+(\lambda_5-\lambda_3)(1-u_2)\frac{\beta_h^{\alpha}I_vS_m}{N_h^2}+(\lambda_6-\lambda_4)(1-u_2)\gamma\frac{\beta_h^{\alpha}I_vS_f}{N_h^2}+\lambda_7\mu_m^{\alpha},\\
{}_tD^{\alpha}_{t_f}\lambda_8 &= (\lambda_2-\lambda_1)\frac{\beta_v^{\alpha}(I_m+I_f)S_v}{N_h^2}+(\lambda_5-\lambda_3)(1-u_2)\frac{\beta_h^{\alpha}I_vS_m}{N_h^2}+(\lambda_6-\lambda_4)(1-u_2)\gamma\frac{\beta_h^{\alpha}I_vS_f}{N_h^2}+\lambda_8\mu_f^{\alpha},
\end{aligned}
$$

which is a fractional system of right Riemann-Liouville derivatives, whose operator is represented by ${}_tD^{\alpha}_{t_f}$. In addition, the following transversality conditions hold:

$$
{}_tD^{\alpha-1}_{t_f}\lambda_i\Big|_{t_f}=0 \iff {}_tI^{1-\alpha}_{t_f}\lambda_i\Big|_{t_f}=\lambda_i(t_f)=0 \qquad i=1,2,...,8,
$$

where ${}_tI^{1-\alpha}_{t_f}$ is the right Riemann-Liouville fractional integer of order $(1-\alpha)$.

7. Forward-Backward Method

The forward-backward method is a widely used iterative numerical technique for solving optimal control problems. It consists of two primary phases: forward integration of the state equations and backward integration of the adjoint (co-state) equations. Through successive iterations, this method refines the control trajectory to minimize the given objective functional effectively. Summarizing the explanations from [28], the procedure can be described as follows:

1. Initialization
   Define the initial conditions for the state variables and the final conditions for the adjoint variables. An initial guess for the control variable $u(t)$ is also specified, which serves as the starting point for the iterative process.
2. Forward Integration
   Solve the state equations from the initial time t_0 to the final time t_f, using the current control variable. This step updates the state variables $x(t)$ over the entire time interval.

3. Backward Integration
   Solve the adjoint equations from t_f back to t_0, using the state variables and control variable obtained from steps 1 and 2. This step updates the adjoint variables $\lambda(t)$ over the time interval.
4. Control Update
   Update the control variable $u(t)$ using state variables $x(t)$ and adjoint variables $\lambda(t)$ obtained from steps 2 and 3.
5. Convergence Check
   Evaluating the difference between the current and previous solutions for the control, state, and adjoint variables. If these differences fall within a predefined tolerance, the iterative process is terminated. Otherwise, the algorithm returns to the forward integration phase, and the process is repeated until convergence is achieved.

8. Numerical Simulation

In this section, we present the numerical simulation to solve the fractional optimal control problem formulated in Section 6. The solution is implemented using a hybrid approach that combines the forward-backward method for optimal control with the Euler's method for solving the fractional differential equations. This hybrid approach provides a robust and efficient framework for addressing complex fractional optimal control problems.

In our numerical simulations, we consider parameter values based on the estimation results, as outlined in Table 3. The initial conditions are specified as follows: $S_v(0) = 50,000,000$, $I_v(0) = 1,000$, $S_m(0) = 21,788,900$, $S_f(0) = 20,641,524$, $I_m(0) = 10,320$, $I_f(0) = 8,819$, $R_m(0) = 0$, and $R_f(0) = 0$, with a convergence check tolerance of 10^{-3}. Furthermore, this study examines three control strategies:

1. **Strategy 1**: Single control using u_1, representing fumigation measures only.
2. **Strategy 2**: Single control using u_2, representing preventive measures only.
3. **Strategy 3**: Combined control using both u_1 and u_2, representing simultaneous application of fumigation and preventive measures.

The simulations are conducted for $t_f = 50$ year, with three different fractional order values: $\alpha = 0.95$, 0.9718, and 1. This allows for an analysis of the impact of fractional order dynamics on the model's behavior under various control scenarios. Figures 4, 5, and 6 display the simulation results for the population of infected mosquito, infected male human and infected female human with and without control for $\alpha = 0.95$, 0.9718, and 1, respectively. By implementing optimal control strategies, there are significant reductions in the numbers of infected mosquitoes, infected male and female individuals compared to without controls. The profile of the optimal control using Strategy 1, Strategy 2, and Strategy 3 for $\alpha = 0.95$, $\alpha = 0.9718$, and $\alpha = 1$ are provided in Figures 7, 8, and 9, respectively.

Table 5. Comparison of the cumulative objective functional for each strategy.

Strategy	$\mathcal{J}$ of $\alpha = 0.95$	$\mathcal{J}$ of $\alpha = 0.9718$	$\mathcal{J}$ of $\alpha = 1$
Single u_1	1.33×10^6	2.20×10^6	4.80×10^6
Single u_2	5.10×10^5	5.26×10^5	5.51×10^5
Combination u_1 and u_2	5.09×10^5	5.24×10^5	5.48×10^5

Table 5 summarizes the values of the cumulative objective functional $(\mathcal{J})$ for three control strategies under different fractional orders. The combined strategy u_1 and u_2 consistently achieves the lowest $\mathcal{J}$ across all fractional orders, indicating that simultaneous implementation of fumigation and prevention is the most effective in reducing the overall system cost. For all strategies, the value of $\mathcal{J}$ increases as the fractional order α increases. This suggests that lower fractional orders result in more efficient system dynamics or reduced system cost.

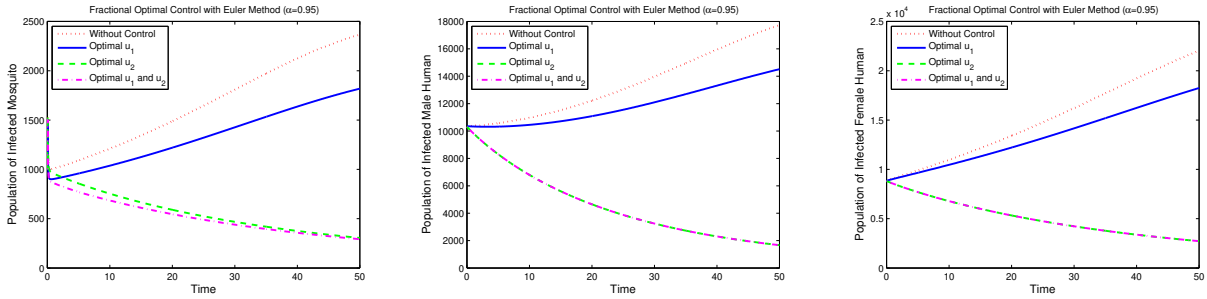

Figure 4. Simulation of fractional optimal control with $\alpha = 0.95$.

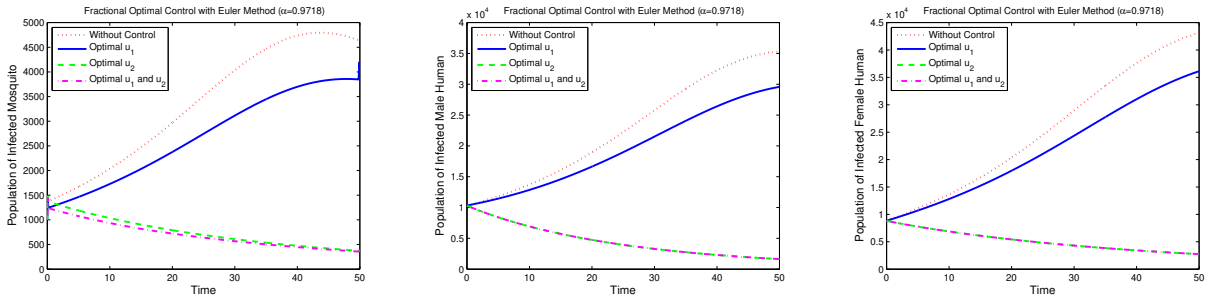

Figure 5. Simulation of fractional optimal control with $\alpha = 0.9718$.

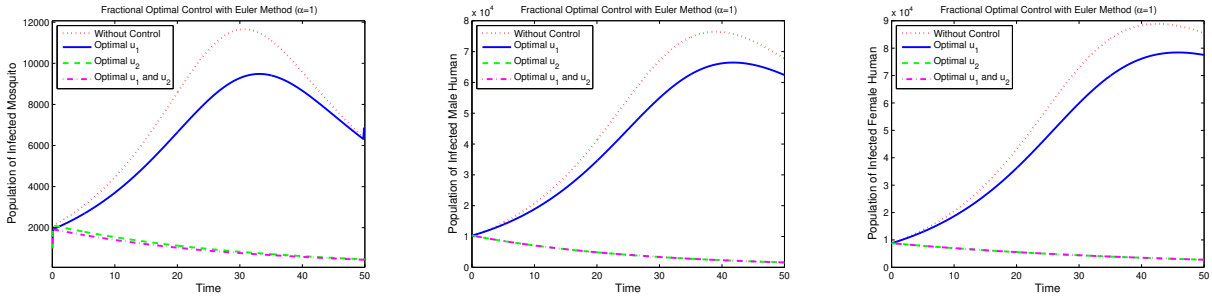

Figure 6. Simulation of fractional optimal control with $\alpha = 1$.

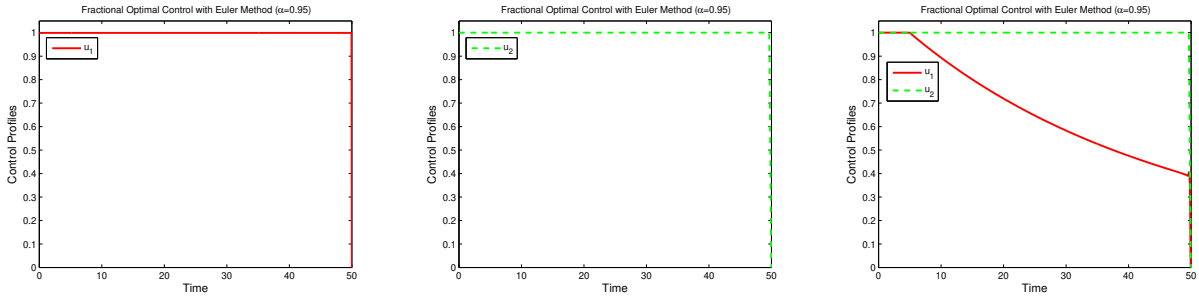

Figure 7. Control profiles of fractional optimal control with $\alpha = 0.95$.

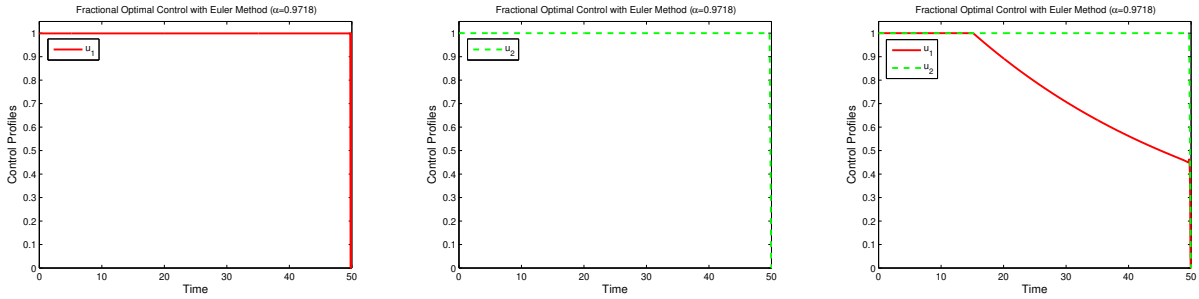

Figure 8. Control profiles of fractional optimal control with $\alpha = 0.9718$.

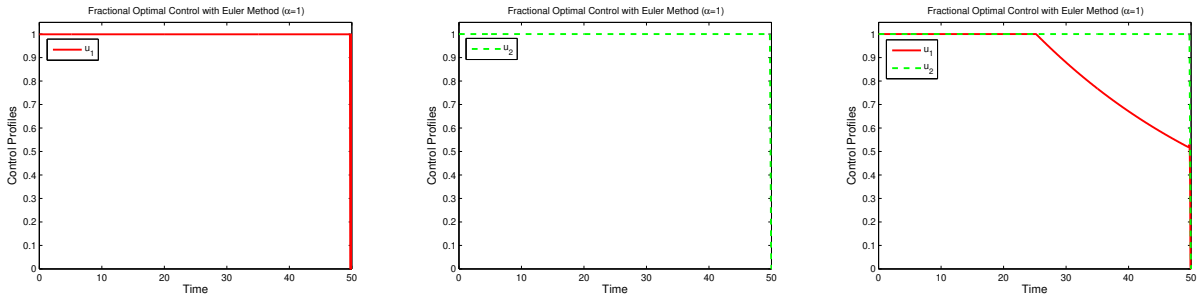

Figure 9. Control profiles of fractional optimal control with $\alpha = 1$.

9. Cost Effectiveness Analysis.

In this section, we assess and compare the advantages and disadvantages of control measures for each method implemented in the previous section. The evaluation is conducted using the Incremental Cost-Effectiveness Ratio (ICER) as a metric. The mathematical definition of ICER, as given in [29], is as follows:

$$\text{ICER} = \frac{\text{Difference in cost produced by strategies } i \text{ and } j}{\text{Difference in the total number of infections averted in strategies } i \text{ and } j}.$$

ICER is used to compare two distinct strategies, denoted as i and j. The numerator represents the difference in intervention costs, which corresponds to the value of the objective function for each strategy, as defined in Table 5. The denominator represents the difference in health outcomes with and without control measures. First, we rank the strategies from the lowest to the highest total number of infections averted. Then, when comparing multiple intervention options, each strategy is evaluated incrementally by comparing it to the next less effective alternative in terms of the overall number of infections prevented. In this study, we only perform cost-effectiveness analysis for $\alpha = 0.9718$, as it represents the best parameter estimation result.

Table 6. Comparison of ICER for each intervention strategies.

Strategies	Optimal Controls	Total Infection Averted	Total Cost	ICER	ICER Recalculated
1	u_1^*	3.429684×10^5	2.20×10^6	6.41	–
2	u_2^*	1.916542×10^6	5.26×10^5	-1.06	0.27
3	u_1^* and u_2^*	1.916544×10^6	5.24×10^5	-1.00	-1.00

The ICER indexes, as reported in Table 6, are obtained as follows.

$$\begin{aligned}
\text{ICER}\,(1) &= \frac{2.20\times10^{6}-0}{3.429684\times10^{5}-0} = 6.41,\\
\text{ICER}\,(2) &= \frac{5.26\times10^{5}-2.20\times10^{6}}{1.916542\times10^{6}-3.429684\times10^{5}} = -1.06,\\
\text{ICER}\,(3) &= \frac{5.24\times10^{5}-5.26\times10^{5}}{1.916544\times10^{6}-1.916542\times10^{6}} = -1.00.
\end{aligned}$$

Comparing Strategy 1 and Strategy 2, the use of Strategy 2 is cost saving over Strategy 1. This indicate the Strategy 1 is less effective and more costly than the other strategy. Hence, Strategy 1 is removed. Furthermore we recalculation the index of ICER as follows.

$$\begin{aligned}
\text{ICER}\,(2) &= \frac{5.26\times10^{5}-0}{1.916542\times10^{6}-0} = 0.27,\\
\text{ICER}\,(3) &= \frac{5.24\times10^{5}-5.26\times10^{5}}{1.916544\times10^{6}-1.916542\times10^{6}} = -1.00.
\end{aligned}$$

Comparing Strategy 2 and Strategy 3, the use of Strategy 3 is cost saving over Strategy 2. This indicate the Strategy 2 is less effective and more costly than the other strategy. Hence, Strategy 2 is removed. Our result suggest that Strategy 3 is the most cost-effective intervention associated with the incremental cost-effectiveness ratio (ICER).

10. Conclusion

The study presented a mathematical model to analyze the dynamics of dengue transmission while incorporating biological and behavioral differences between male and female humans. By employing fractional calculus, the model accounts for memory effects, which are essential in capturing the long-term dynamics of diseases. The inclusion of control variables, representing fumigation and preventive measures, allows for the evaluation of effective intervention strategies. The fractional-order approach enhances the realism of the model, offering better predictions compared to classical integer-order models. Furthermore, the differentiation between male and female populations highlights critical biological and immunological differences, enabling the design of more targeted interventions.

This study successfully formulated a fractional optimal control problem, applying Pontryagin's Minimum Principle and the forward-backward numerical method to determine optimal control strategies, while Euler's method was utilized for solving the fractional differential equations. Numerical simulations demonstrated that lower fractional orders enhance the efficiency of system dynamics, leading to faster infection reduction. Sensitivity analysis revealed that key parameters, particularly the proportion of additional immunity levels among females, significantly influence disease spread. Simulation results showed that increasing this parameter reduces female infections, subsequently lowering vector transmission and indirectly decreasing male infections.

Among the evaluated intervention strategies, the combined approach simultaneous implementation of fumigation and preventive measures proved to be the most effective, achieving the lowest infection levels and cost strategies. The cost-effectiveness analysis further confirmed this strategy as the most efficient in balancing disease control and intervention costs.

This research provides valuable insights for understanding and mitigating dengue transmission through a fractional epidemiological model that incorporates sex specific dynamics. The fractional optimal control framework offers a practical tool for public health policymakers to design cost effective interventions. Future studies could expand on this work by considering additional real world factors, such as seasonal variations, vector resistance to fumigation, and socioeconomic impacts, to enhance the model's relevance and applicability.

REFERENCES

1. World Health Organization, *Dengue and severe dengue*, 2024, Accessed: Jan. 06, 2025. Available: https://www.who.int/news-room/fact-sheets/detail/dengue-and-severe-dengue.
2. S. L. Klein, *The effects of hormones on sex differences in infection: from genes to behavior*, Neuroscience and Biobehavioral Reviews, vol. 24, no. 6, pp. 627–638, 2020.
3. I. Podlubny, *Fractional Differential Equations, Mathematics in Science and Engineering*, vol. 198. San Diego, California, USA: Academic Press, 1999.
4. E. Bonyah, M. L. Juga, C. W. Chukwu, and Fatmawati, *A fractional order dengue fever model in the context of protected travelers*, Alexandria Engineering Journal, vol. 61, no. 1, pp. 927–936, 2022.
5. J. K. K. Asamoah, and Fatmawati, *A fractional mathematical model of heartwater transmission dynamics considering nymph and adult amblyomma ticks*, Chaos, Solitons & Fractals, vol. 174, 113905, 2023.
6. S. A. Jose, Z. Yaagoub, D. Joseph, R. Ramachandran, and A. Jirawattanapanit, *Computational dynamics of a fractional order model of chickenpox spread in Phuket province*, Biomedical Signal Processing and Control, vol. 91, 105994, 2024.
7. F. F. Herdicho, S. A. Jose, A. Jirawattanapanit, and T. Park, *Fractional derivative model in COVID-19 dynamics: application to symptom severity and hospital resource allocation in South Korea*, Journal of Applied Mathematics and Computing, 2025.
8. S. Rosa, and D. F. M. Torres, *Parameter Estimation, Sensitivity Analysis and Optimal Control of a Periodic Epidemic Model with Application to HRSV in Florida*, Statistics, Optimization and Information Computing, vol. 6, no. 1, 2018.
9. D. Aldila, N. Awdinda, Fatmawati, F. F. Herdicho, M. Z. Ndii, and C. W. Chukwu, *Optimal control of pneumonia transmission model with seasonal factor: Learning from Jakarta incidence data*, Heliyon, vol. 9, no. 7, e18096, 2023.
10. Fatmawati, C. W. Chukwu, R. T. Alqahtani, C. Alfiniyah, F. F. Herdicho, and Tasmi, *A Pontryagin's maximum principle and optimal control model with cost-effectiveness analysis of the COVID-19 epidemic*, Decision Analytics Journal, vol. 8, 100273, 2023.
11. J. Nainggolan, M. F. Ansori, and H. Tasman, *An optimal control model with sensitivity analysis for COVID-19 transmission using logistic recruitment rate*, Healthcare Analytics, 100375, 2025.
12. B. A. Baba, and B. Bilgehan, *Optimal control of a fractional order model for the COVID – 19 pandemic*, Chaos, Solitons & Fractals, vol. 144, 110678, 2021.
13. S. Rosa, and D. F. M. Torres, *Numerical Fractional Optimal Control of Respiratory Syncytial Virus Infection in Octave/MATLAB*, Mathematics, vol. 11, no. 6, 1511, 2023.
14. H. R. Pandey, G. R. Phaijoo, and D. B. Gurung, *Dengue dynamics in Nepal: A Caputo fractional model with optimal control strategies*, Heliyon, vol. 10, no. 13, e33822, 2024.
15. B. Diallo, M. Dasumani, J. A. Okelo, S. Osman, O. Sow, N. S. Aguegboh, and W. Okongo, *Fractional optimal control problem modeling bovine tuberculosis and rabies co-infection*, Results in Control and Optimization, vol. 18, 100523, 2025.
16. L. B. Dano, D. G. Gobena, L. L. Obsu, M. H. Dangisso, and M. H. Kidanie, *Fractional modeling of dengue fever with optimal control strategies in Dire Dawa, Ethiopia*, Scientific African, vol. 27, e02500, 2025.
17. C. Li, and F. Zeng, *Numerical Methods for Fractional Calculus*, New York: Chapman and Hall/CRC, 2015.
18. K. Diethelm, N. J. Ford, A. D. Freed, and Y. Luchko, *Algorithms for the fractional calculus: A selection of numerical methods*, Computer Methods in Applied Mechanics and Engineering, vol. 194, no. 6-8, pp. 743–773, 2005.
19. Open Data West Java Province, Indonesia, *Jumlah kasus demam berdarah dengue (DBD) berdasarkan jenis kelamin di jawa barat*, 2022, Accessed: May 25, 2024. Available: https://opendata.jabarprov.go.id/id/dataset/jumlah-kasus-demam-berdarah-dengue-dbd-berdasarkan-jenis-kelamin-di-jawa-barat.
20. Open Data West Java Province, Indonesia, *Jumlah kasus meninggal demam berdarah dengue (DBD) berdasarkan jenis kelamin di jawa barat*, 2022, Accessed: May 25, 2024. Available: https://opendata.jabarprov.go.id/id/dataset/jumlah-kasus-meninggal-demam-berdarah-dengue-dbd-berdasarkan-jenis-kelamin-di-jawa-barat.
21. Open Data West Java Province, Indonesia, *Jumlah penduduk berdasarkan jenis kelamin di jawa barat*, 2022, Accessed: May 25, 2024. Available: https://opendata.jabarprov.go.id/id/dataset/jumlah-penduduk-berdasarkanjenis-kelamin-dan-kabupatenkota-di-jawa-barat.
22. Central Bureau of Statistics, Indonesia, *Angka harapan hidup (AHH) menurut provinsi dan jenis kelamin (tahun)*, 2023, Accessed: May 25, 2024. Available: https://www.bps.go.id/id/statistics-table/2/NDU1IzI=/angkaharapan-hidup--ahh--menurut-kabupaten-kota-dan-jenis-kelamin.html.
23. M. Samsuzzoha, M. Singh, and D. Lucy, *Parameter estimation of influenza epidemic model*, Applied Mathematics and Computation, vol. 220, pp. 616–629, 2013.
24. I. Mahmood, M. Jahan, D. Groen, A. Javed, and F. Shafait, *An agent-based simulation of the spread of dengue fever*, Computational Science-ICCS 2020: 20^{th} International Conference, vol. 12139, pp. 103–117, 2020.
25. N. Chitnis, J. M. Hyman, and J. M. Cushing, *Determining important parameters in the spread of malaria through the sensitivity analysis of a mathematical model*, Bulletin of Mathematical Biology, vol. 70, pp. 1272–1296, 2008.
26. P. Van den Driessche, and J. Watmough, *Reproduction numbers and sub-threshold endemic equilibria for compartemental models of disease transmission*, Mathematical Biosciences, vol. 180, pp. 29–48, 2002.
27. L. S. Pontryagin, *Mathematical Theory of Optimal Processes*, New York: John Wiley & Sons, 1987.
28. S. Lenhart and J. T. Workman, *Optimal Control Applied to Biological Models*, New York: Chapman and Hall/CRC, 2007.
29. B. Buonomo, and R. D. Marca, *Optimal bed net use for a dangue disease model with mosquito seasonal pattern*, Mathematical Methods in the Applied Sciences, vol. 41, no. 2, pp. 573–592, 2017.